2023 IEEE International Conference on Robotics and Automation (ICRA 2023)
May 29 - June 2, 2023. London, UK

Autonomous Underwater Docking using Flow State Estimation and Model Predictive Control

Rakesh Vivekanandan, Dongsik Chang, and Geoffrey A. Hollinger

***Abstract*— We present a navigation framework to perform autonomous underwater docking to a wave energy converter (WEC) under various ocean conditions by incorporating flow state estimation into the design of model predictive control (MPC). Existing methods lack the ability to perform dynamic rendezvous and autonomously dock in energetic conditions. The use of exteroceptive sensors or high performing acoustic sensors have been previously investigated to obtain or estimate the flow states. However, the use of such sensors increases the overall cost of the system and expects the vehicle to navigate close to the seafloor or other landmarks. To overcome these limitations, our method couples an active perception framework with MPC to estimate the flow states simultaneously while moving towards the dock. Our simulation results demonstrate the robustness and reliability of the proposed framework for autonomous docking under various ocean conditions. Furthermore, we conducted laboratory trials with a BlueROV2 docking with an oscillating dock and achieved a greater than 70% success rate.**

I. Introduction

The capabilities of marine vehicles, such as autonomous underwater vehicles (AUVs) and remotely-operated vehicles (ROVs), have significantly advanced to perform complicated operations such as navigating through unexplored and dynamic environments, inspection of underwater structures, and monitoring of ocean conditions in deep waters. However, the limited energy resources of AUVs and tethered connectivity of ROVs constrain survey lengths and subsequently increase the operational costs. Underwater docking stations that can recharge vehicles and transmit their data offer a potential solution to extend the endurance of vehicles.

Motion planning for underwater docking is a difficult and unsolved problem as it involves understanding the dynamics of various components of the system and the environmental factors influencing the vehicle's motion. Offline trajectory planning is often challenging given the dynamic nature of an underwater environment, even though offline strategies are effective in ideal circumstances. Ocean currents and waves can negatively impact the AUV's actual path, causing it to deviate and not be able to reach the dock.

The ability to perform dynamic rendezvous and autonomously dock in energetic environments is missing from existing systems. In most prior work [1]–[12], ocean current information is either obtained through exteroceptive sensors or is estimated using Doppler Velocity Logger (DVL) or other acoustic sensors. This not only increases the overall cost of the system but also restricts the operational workspace of the vehicle by expecting it to be in close proximity to landmarks or the seafloor. To overcome this limitation, we formulate the docking problem using an active perception framework and generate trajectories for a 6-DOF marine vehicle using a multi-objective optimization (MOO) approach.

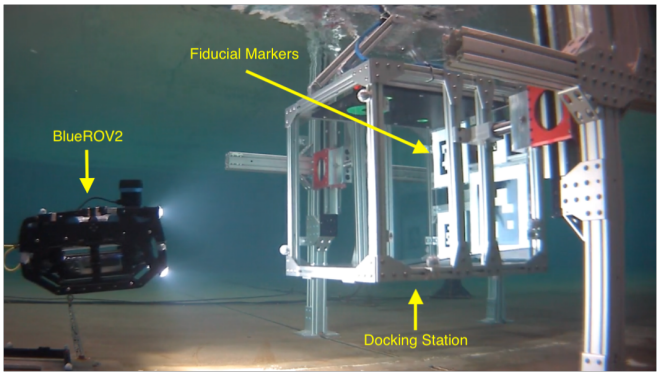

Fig. 1: BlueROV2 underwater vehicle autonomously docking using the proposed model predictive control algorithm with an oscillating docking station.

As a main contribution, we present a navigation framework that couples flow state estimation with model predictive control (MPC) to perform autonomous underwater docking to a wave energy converter (WEC) under various ocean conditions. The proposed method allows for robust AUV docking and recharging in real-world conditions. Our proposed method outperforms the state-of-the-art techniques used for autonomous docking in the presence of ocean current disturbances. Additionally, we conducted laboratory trials with a BlueROV2 and were able to dock reliably with a docking station actuated with heave motion (see Fig. 1). Preliminary versions of this algorithm were presented in our previous workshop paper [13] and poster [14].

II. Related Works

Path planning and trajectory optimization are significant components of autonomous underwater docking. Hernandez et al. [15] present a framework for an AUV to navigate and reach a goal location, through unexplored environments. But they do not consider the non-linearity of the environment or the uncertainty of estimates of the state. Following Findeisen et al. [16], a real-time control of an AUV, based on MPC, is introduced in Medagoda et al. [17]. The objective is to perform trajectory tracking in a water column using an

This research is supported by the U.S. Department of Energy's Office of Energy Efficiency and Renewable Energy (EERE) under FOA2234 Topic Area 1: Marine Energy Foundational Research and Testing Infrastructure, DE-EE0009449.

R. Vivekanandan and G.A. Hollinger are with the Collaborative Robotics and Intelligent Systems Institute (CoRIS), Oregon State University, Corvallis, OR, 97331, USA. (emails: {vivekanr, geoff.hollinger}@oregonstate.edu)

D. Chang was with CoRIS, Oregon State University, Corvallis, OR, 97331, USA. (email: dongsikc3@gmail.com)

MPC that accounts for the water current estimates from the ADCP-aided localization filter. In Fernandez et al. [18], an MPC is used to achieve the station-keeping application of a marine vehicle in ocean waves. The state estimator design employs Linear Wave Theory (LWT) to forecast and adjust the vehicle's state for the wave action.

The application of MPC to underwater robotics is a promising approach as it requires minimal tuning of the controller. The MPC-based 3D trajectory tracking strategy designed in Zhang et al. [19] translates the system's state constraints into input constraints and transforms the optimization problem into quadratic programming (QP). Wallen et al. [20] present a finite horizon MPC to verify the concept of docking to a dynamic platform whose motion pattern is very similar to that of an offshore WEC. Although the methods presented in Yan et al. [21] and Cao et al. [22] account for external disturbances while designing the MPC, they do not utilize the complete model of vehicle dynamics. This limitation is addressed in our previous workshop paper [13], which complements Wallen et al. [20] by seeking a more comprehensive numerical framework further connecting the environmental disturbances experienced by the docking station to the robotic motion planning problem. A common assumption made in [13], [20]–[22] is that they have the true characteristics of ocean currents. However, perfect ocean current information is unavailable.

The likelihood that autonomous docking would succeed can be increased by acquiring the ability to estimate unknown current disturbances and adjust the docking maneuvers. In most prior work, it is demonstrated that underwater navigation is supported by reasonable estimation of ocean currents, in the presence of DVL or other acoustic sensors [1]–[12]. However, such sensors provide useful information only if the vehicle is in close proximity to the sea floor or other landmarks. They are expensive and may require transponders to be attached to surface vessels or on submerged structures, which subsequently increases operational costs. In more recent work, Chang et al. [23] present an active perception framework that improves flow state estimation and vehicle navigation without using any exteroceptive sensors, such as DVLs, USBLs, and other acoustic sensors.

In this paper, we present a navigation framework that incorporates flow state estimation [23] into the design of MPC [13], [14] for robust and reliable autonomous docking.

III. Preliminaries

A. Vehicle Motion Model

In this paper, we use a six degrees-of-freedom vehicle motion model to design vehicle control in the presence of ocean disturbances. The model uses two reference frames: The inertial frame (earth-fixed) $\{n\}$, coincidental with the North-East-Down (NED) coordinate system, and the body-fixed frame $\{b\}$. Let us denote the position and orientation of the vehicle in $\{n\}$ by $\eta_1 = [x, y, z]^T \in \mathbb{R}^3$ and $\eta_2 = [\phi, \theta, \psi]^T \in \mathbb{R}^3$, respectively. Together, the pose of the vehicle is defined by $\eta = [\eta_1^T, \eta_2^T]^T \in \mathbb{R}^6$. With the vehicle linear and angular velocity denoted in $\{b\}$ by $\nu_1 = [u, v, w]^T \in \mathbb{R}^3$ and $\nu_2 = [p, q, r]^T \in \mathbb{R}^3$, respectively, the velocity of the vehicle is represented by $\nu = [\nu_1^T, \nu_2^T]^T \in \mathbb{R}^6$. Then, vehicle motion can be described by

$$\dot{\eta} = J(\Theta)\nu \tag{1}$$

$$M_{RB}\dot{\nu} + M_A\dot{\nu_r} + C_{RB}(\nu)\nu + C_A(\nu_r)\nu_r + D(\nu_r)\nu_r + g(\eta) = \tau, \tag{2}$$

where $\nu_r = [\nu_{r_1}^T, \nu_{r_2}^T]^T = \nu - \nu_c \in \mathbb{R}^6$ represents the vehicle velocity relative to ocean flow velocity $\nu_c = [\nu_{c_1}^T, \nu_{c_2}^T]^T \in \mathbb{R}^6$; $J(\Theta)$ is a transformation matrix from $\{b\}$ to $\{n\}$ with respect to vehicle orientation Θ; $M_{RB} \in \mathbb{R}^{6\times6}$ and $M_A \in \mathbb{R}^{6\times6}$ are the rigid body and added masses; $C_{RB} \in \mathbb{R}^{6\times6}$ and $C_A \in \mathbb{R}^{6\times6}$ are Coriolis and centripetal terms due to the rigid body and added masses, respectively; $D \in \mathbb{R}^{6\times6}$ and $g(\eta) \in \mathbb{R}^6$ represent the hydrodynamic damping and the hydrostatic restoring forces, respectively; and $\tau \in \mathbb{R}^6$ represents the forces and moments acting on the vehicle.

Eqs. (1) and (2) represent the vehicle kinematics and dynamics, respectively. For brevity, we refer the readers to [24] for details about the model. Let us define vehicle state vector $\mathbf{x} = [\eta^T, \nu^T]^T \in \mathbb{R}^{12}$ and control input $\mathbf{u} \in \mathbb{R}^8$ for our testbed vehicle that satisfies $\tau = B\mathbf{u}$, where B is the thruster allocation matrix. In this paper, we assume irrotational flow velocity (i.e., $\dot{\nu_{c_2}} = 0$). With this assumption, a discretized vehicle motion model is given by

$$\mathbf{x}(k+1) = f(\mathbf{x}(k), \mathbf{u}(k)), \tag{3}$$

where f represents the discretized vehicle motion derived from (1) and (2). Details of the model is presented in the next section.

In this work, a BlueROV2 Heavy is used as the testbed vehicle for simulations. The rigid body and hydrodynamics coefficients of the vehicle are obtained from [25]. BlueROV2 Heavy is controllable in 6 DOF by a combination of eight thrusters. While the proposed framework is demonstrated using a BlueROV2 Heavy, we note that the framework can be implemented on similarly actuated underwater vehicles whose system parameters can be identified.

B. Flow Motion Model

Let us express ocean flow velocity ν_c with its linear and angular components defined as $\nu_{c_1} = [u_c, v_c, w_c]^T \in \mathbb{R}^3$ and $\nu_{c_2} = [p_c, q_c, r_c]^T \in \mathbb{R}^3$, respectively. In this work, we represent the ocean flow by assuming an irrotational flow field, a widely used assumption in the literature [24], as the vehicle does not stay at a fixed position.

$$\dot{\nu_{c_1}} = -\mathbf{S}(\nu_2)\nu_{c_1} = -\mathbf{S}(\nu_{r_2})\nu_{c_1} \tag{4}$$

$$\dot{\nu_{c_2}} = 0, \tag{5}$$

where $\mathbf{S}$ is a skew symmetric matrix. Flow estimation is constructed based on the above model but aims to estimate time-varying flow. We evaluate the performance of the presented controller on ocean flow varying in space and time such as double-gyre flow.

For an irrotational flow velocity, Eq. (2) can be simplified to describe vehicle motion relative to the ocean flow as

$$M\dot{\nu_r} + C(\nu_r)\nu_r + D(\nu_r)\nu_r + g(\eta) = \tau. \tag{6}$$

C. Wave Energy Converter (WEC) Motion Model

To analyze the feasibility of the proposed strategy for docking, the simulated WEC is limited to only translatory heave motion with sinusoidal oscillations. This represents the predominant motion typically seen by docks in ocean waves [26]. Let us define WEC state vector $\mathbf{x}_W \in \mathbb{R}^{12}$ whose vertical motion is described by

$$\dot{z}_W = \omega A cos(\omega t), \tag{7}$$

where ω and A are the frequency and amplitude of oscillation, respectively.

IV. Problem Formulation

A closed-loop MPC is coupled with flow state estimation to present a navigation framework for autonomous underwater docking.

Assumption 1: True vehicle state is available during the entire docking operation (e.g. using an acoustic positioning system or other localization methods).

Assumption 2: The location of the WEC relative to the vehicle is available during the entire docking operation.

A. Flow State Estimation

Unknown background flow can cause perturbations to an underwater vehicle's motion, leading to an unsuccessful attempt at docking. In this paper, we integrate the approach presented in [23], which considers the coupling between vehicle motion and ocean currents to facilitate flow state estimation, for reliable docking with fewer failures.

Uniform complete observability of the flow state, along the vehicle trajectory, is maintained by obtaining a control input that minimizes the maximum variance of the flow state estimation. To facilitate this, $\mathcal{F}$ is defined as the information metric, that corresponds to the observability and performance of the flow state estimation, and can be described as

$$\mathcal{F} = \lambda_{min}(\mathcal{G}_{cg}^{\nu_{c1}}(-\infty, k+1)), \tag{8}$$

where $\nu_{c1} \in \mathbb{R}^3$ represents the linear component of the flow velocity, $\lambda_{min}(.)$ denotes the smallest eigenvalue of (.) and $\mathcal{G}_{cg}^{\nu_{c1}}$ represents the constructability gramian of the linearly time-varying ocean flow system.

The control law pertaining to flow state estimation can be defined as

$$\begin{aligned} \tau_k^\star &= \underset{\tau_k}{\operatorname{argmax}}\, \mathcal{F} \\ &\text{subject to } (6), \tau_{min} \leq \tau_k \leq \tau_{max}, \end{aligned} \tag{9}$$

where $\tau_k^\star$ is the active perception control input.

A Kalman filter is specifically designed for the purpose of predicting and estimating ocean currents. The Kalman filter for flow state estimation uses inertial sensor measurement as observation and we provide that given a perfectly known vehicle state with noise. For details on the design of the Kalman filter, we refer the readers to [23].

B. Optimal Control

We present a navigation framework that incorporates flow state estimation into the MPC formulation for a more reliable and robust docking approach. This is accomplished by modifying the objective function to include the information metric, defined in (8).

At time $k = \kappa$, the optimal control problem seeks to find a sequence of $N+1$ optimal control inputs $\mathbf{U}^\star = \{\mathbf{u}^\star(0), \cdots, \mathbf{u}^\star(N)\}$ by minimizing the objective function J such that

$$\begin{aligned} \mathbf{U}^\star = \underset{\{\mathbf{u}(0),\cdots,\mathbf{u}(N)\}}{\operatorname{argmin}} J = \sum_{k=\kappa}^{t+N-1} \Big[\|\mathbf{x}(k) - \mathbf{x}_W(k)\|_Q^2 \\ + \|\mathbf{u}(k+1) - \mathbf{u}(k)\|_R^2 - \alpha\mathcal{F}\Big] + \|\mathbf{x}(N) - \mathbf{x}_W(N)\|_P^2 \\ \text{subject to } (3),\ \mathbf{x}(0) = \mathbf{x}_0,\ \mathbf{x}_{min} \leq \mathbf{x}(k) \leq \mathbf{x}_{max}, \\ \mathbf{u}_{min} \leq \mathbf{u}(k) \leq \mathbf{u}_{max}, \end{aligned} \tag{10}$$

where $\mathbf{x}_W \in \mathbb{R}^{12}$ represents the WEC state vector, N is the prediction horizon, α is a scalarization factor and P, Q, and R are the weight matrices for terminal error cost, accumulated error cost, and control discontinuity cost, respectively.

The key significance of the proposed approach is that it enables the vehicle to counter the influence of unknown flow disturbances while simultaneously moving closer to the docking station, in an optimal manner.

V. Methods

In this section, we present the overview of the proposed navigation frameworks for autonomous docking. As described above, motion planning for underwater environments is difficult due to multiple factors, such as the effect of waves and currents on the vehicle's motion, poor vehicle localization, sensor limitations, among others. Our work focuses particularly on simultaneously estimating the ocean currents and compensating its influence while performing autonomous docking. To demonstrate this, we formulate the navigation framework in the following two ways:

- Combined optimization of flow state estimation and docking trajectory (Optimized FSE-MPC)
- Sequential optimization of flow state estimation and docking trajectory (Sequential FSE-MPC)

A. Optimized FSE-MPC

In this method, we use a weighted-sum scalarization approach to approximate the MOO problem of simultaneously estimating the flow state and planning the AUV's docking trajectory. The α term in (10) is the weight associated with the information metric for flow state estimation. Given the vehicle's current state and target state, we obtain a sequence of $N+1$ optimal control inputs $\mathbf{U}^\star = \{\mathbf{u}^\star(0), \cdots, \mathbf{u}^\star(N)\}$ by solving the optimization defined in (10). In our implementation, only the first control action $\mathbf{u}^\star(0)$ in $\mathbf{U}^\star$ is executed. While the vehicle is in motion, we generate inertial sensor measurements based on the vehicle's state and use them as a measurement for correcting the Kalman filter. Following

which, the flow states are predicted for the next time step. This process is repeated until the vehicle successfully docks.

B. Sequential FSE-MPC

Due to the computational requirement for MOO, Optimized FSE-MPC is computationally expensive. To overcome this, we designed an alternate strategy that solves the objectives sequentially, one after the other. At each time step, the active perception control input is obtained by solving the control law defined in (9). It is then added to the MPC optimization variable $\mathbf{U}$, to maintain uniform complete observability of the flow state along the docking trajectory. Before solving for the optimal control input, we define $\alpha = 0$ to disable MOO. Following this step, the algorithm adheres to the same procedure as Optimized FSE-MPC and is repeated until successful docking is achieved.

C. Baseline Methods

Three baseline approaches are implemented, and their performance is evaluated in various ocean conditions. All of them utilize the same cost function J defined in (10) with $\alpha = 0$, to disable MOO. The key difference between the methods is the formulation of kinematic and dynamic models of the vehicle.

Assumption 3: True flow state is measured using exteroceptive sensors and is available during the entire docking operation for the Kinematic MPC and Oracle MPC.

1) Naive MPC: This controller does not consider the effect of ocean currents in the vehicle motion model. Substituting $\nu_c = 0$ into (1), it becomes

$$\dot{\eta} = J(\Theta)\nu_r. \tag{11}$$

The simplified vehicle motion model follows (11) and (6).

2) Kinematic MPC (K-MPC): In this method, the effect of ocean currents is only considered in the kinematic equation (1). To understand the performance of the controller purely with respect to the kinematics of the vehicle, a simplified dynamic model (6) is utilized.

3) Oracle MPC: Following Assumption (3), access to ocean current information allows this method to utilize the complete vehicle motion model as defined in (3). The key difference between this and the proposed algorithms is that it does not estimate the flow states. We note that it is not feasible to implement this algorithm in real-time without perfect information on ocean currents.

VI. Algorithm Layout

Algorithm 1 shows the procedure for the proposed frameworks (Optimized and Sequential FSE-MPC). The algorithm requires two inputs, namely the current state of the vehicle and its target state. Once all inputs are passed through, the designed Kalman filter is initialized with a rough estimate of the flow state. Following which, the MPC is initialized. Then, until the vehicle reaches the dock successfully, MPC obtains a sequence of optimal control input $\mathbf{U}^\star$ based on the type of framework used, executes the first control action $\mathbf{u}^\star(0)$ from the sequence and performs Kalman filter correction and prediction of the flow states, at the end of each iteration. If the chosen framework is the multi-objective Optimized FSE-MPC, α is set to 10^{-15} to appropriately scale $\mathcal{F}$ with respect to the objective function mentioned in (10). Then the controller minimizes (10) to obtain the optimal control input. Otherwise, if the chosen framework is Sequential FSE-MPC, α is set to 0 to disable MOO. Then the optimal control associated with active perception $\tau_k^\star$ is separately obtained and added to the MPC optimization variable $\mathbf{U}$ prior to minimizing (10) for the optimal control input.

Algorithm 1 Navigation Framework for Autonomous Underwater Docking

Input: Current state, Target state
Initialize Kalman filter with an estimate of flow state
Initialize MPC
repeat
  if Optimized FSE-MPC **then**
    $\alpha = 10^{-15}$ ▷ Enable MOO
  else
    if Sequential FSE-MPC **then**
      $\alpha = 0$ ▷ Disable MOO
      $\tau_k^\star = \text{argmax}_{\tau_k} \mathcal{F}$
      Add $\tau_k^\star$ to the MPC optimization variable $\mathbf{U}$
    end if
  end if
  $\mathbf{U}^\star = \{\mathbf{u}^\star(0), \cdots, \mathbf{u}^\star(N)\} \leftarrow (10)$ ▷ Optimization
  $\mathbf{u}^\star \leftarrow \mathbf{u}^\star(0)$
  Propagate the vehicle using $\mathbf{u}^\star$
  Kalman filter correction for flow state
  Kalman filter prediction for flow state
until AUV reaches dock successfully

Algorithm 2 shows the procedure for Oracle MPC. The algorithm requires two inputs, namely the current state of the vehicle and its target state. Once all inputs are passed through, α is set to 0 and the MPC is initialized. Then, until the cessation criteria are satisfied, periodically update the flow states based on the known data, obtain the optimal control sequence $\mathbf{U}^\star$ and execute the first control action $\mathbf{u}^\star(0)$ from the sequence.

Algorithm 2 Oracle MPC

Input: Current state, Target state
$\alpha = 0$ ▷ Disable MOO
Initialize MPC
repeat
  Update flow state based on the known data
  $\mathbf{U}^\star = \{\mathbf{u}^\star(0), \cdots, \mathbf{u}^\star(N)\} \leftarrow (10)$ ▷ Optimization
  $\mathbf{u}^\star \leftarrow \mathbf{u}^\star(0)$
  Propagate the vehicle using $\mathbf{u}^\star$
until AUV reaches dock successfully

VII. Simulations

The methods described in Section V were implemented in Python using the Casadi optimization library [27] and was run on a laptop with an Intel i7-10870H CPU.

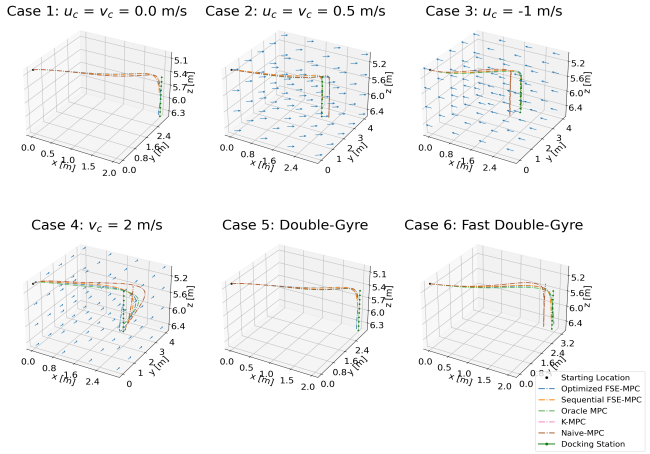

Fig. 2: Vehicle docking trajectories from different algorithms under various ocean conditions. Optimized and Sequential FSE-MPC converge to the dock in all cases, similarly to the Oracle. However, K-MPC and Naive-MPC do not.

A. Simulation Setup

1) Ocean Flow Models: Ocean flow models can be broadly categorized as constant and time-varying flow fields. In this work, we simulate six different environmental flow conditions to evaluate the robustness and reliability of using the proposed navigation framework for autonomous docking. Simulated constant flow conditions can be defined as: $u_c = v_c = 0\ m/s$, $u_c = v_c = 0.5\ m/s$, $u_c = -1\ m/s$ and $v_c = 2\ m/s$. Recall that u_c, v_c are the linear flow velocities along the surge and sway axes, respectively. A two-dimensional (2D) double-gyre pattern [28], is simulated to evaluate the performance of the proposed navigation framework under time-varying flow field conditions. Here, we use $\mathcal{A} = 0.1/\pi$ as the magnitude of flow velocity, $\omega = 2\pi/T$ as the frequency of oscillation, and $T = 12h$ as the total time period. The AUV's operational domain is translated to [-7.5 km, 12.5 km] x [-7.5 km, 2.5 km]. Furthermore, we use $\mathcal{A} = 0.5$ and $T = 6h$ to simulate a larger and frequently changing double-gyre pattern.

Assumption 4: A uniform flow field exists along the z-axis i.e., $w = 0$.

We extend the flow field to three-dimensional (3D) space following Assumption 4 in all of the above-listed cases.

2) MPC Design Parameters: We empirically chose a time step $dt = 0.05\ s$, a prediction horizon window $N = 10$, and a convergence tolerance for docking with a precision of 0.05 units. For simulations, the vehicle starts at $(x, y, z) = (0, 0, 5)$ facing true North 0°and navigates until it meets the dock oscillating at $(x_W, y_W) = (2, 3)$ in the z axis with the target heading of 0°.

B. Results and Discussion

Fig. 2 illustrates the comparison of optimized paths from different algorithms under various ocean conditions. Across all cases, Oracle MPC, Sequential and Optimized FSE-MPC are able to reach the docking station successfully. However, Naive MPC and K-MPC only perform successful homing under still water or calm conditions (Cases: 1, 5). In stronger flow conditions (Cases: 2-4, 6), Navie MPC and K-MPC are

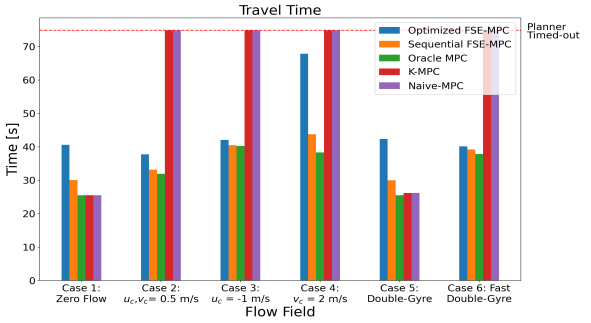

Fig. 3: Travel time of vehicle using different algorithms under various ocean conditions.

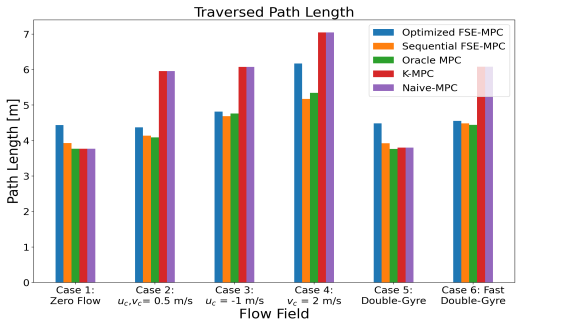

Fig. 4: Length of path traversed by the vehicle using different algorithms under various ocean conditions.

unable to counter the effect of ocean currents. Irrespective of the controller used, the vehicle first moves to the top position of the vertical trajectory of the dock. Since the WEC is constantly moving, the vehicle follows the dock and achieves docking at the position of the trajectory where the convergence tolerance for docking is satisfied.

Fig. 3 demonstrates the comparison of the time taken by the vehicle to reach the docking station using the discussed methods under various ocean conditions. As stated earlier, in strong ocean conditions (Cases 2-4, 6), Naive MPC and K-MPC fail to reach the desired location and eventually the planners get timed out at 75 s. On the other hand, under similar flow conditions (Cases 2-4, 6), it can be noted that Oracle MPC, Sequential, and Optimized FSE-MPC are successful. The key observation is that our proposed methods (Sequential and Optimized FSE-MPC) take longer than the Oracle MPC as the vehicle needs to explore the environment in order to maintain uniform complete observability of the flow states along the docking trajectory. The vehicle takes the longest time with Optimized FSE-MPC, under all flow conditions, because the optimization of the two objectives, namely flow state estimation and generation of optimal docking trajectory, are tightly coupled and the controller tries to find the Pareto optimal solution. On the contrary, controlling the vehicle using Sequential FSE-MPC results in shorter travel time as the controller prioritizes generating an optimal trajectory over estimating flow states.

We also evaluate the length of the path traversed (see Fig. 4) and the performance of flow state estimation (see Fig. 5) under various flow conditions. Since Naive MPC and

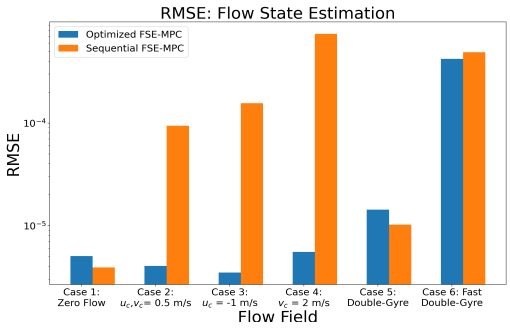

Fig. 5: Performance comparison of flow state estimation. Optimized FSE-MPC provides better estimation of flow states, but at a significantly higher computational cost.

K-MPC do not converge under strong flow fields (Cases 2-4, 6) the corresponding path lengths are significantly longer than the other algorithms. Although Oracle MPC has perfect knowledge of the flow states based on Assumption 3, the vehicle reaches the docking station in a relatively shorter path when controlled with Sequential FSE-MPC, for Cases 3 and 4. This can be substantiated by the high root mean squared error (RMSE) of Sequential FSE-MPC as seen in Fig. 5. Since it is biased toward generating an optimal docking trajectory, it restricts the exploration of states in the environment for better flow state estimation. As a result, the optimal control input from Sequential FSE-MPC drives the vehicle into states that are closer to the dock than Oracle MPC. On the other hand, Optimized FSE-MPC produces lower values of RMSE, and longer paths compared to Sequential FSE-MPC. Additionally, it was found that the average computational time for Optimized FSE-MPC was $5014.83\ s$ when compared to $203.08\ s$ for Sequential FSE-MPC across all the cases. From Fig. 5, it can be inferred that the performance of both algorithms is relatively the same for cases 1, 5, and 6. But for stronger constant ocean currents (Cases 2, 4), Sequential FSE-MPC has a higher RMSE than the Optimized FSE-MPC due to the restricted exploration.

VIII. Experiments

A. Experimental Setup

For experimental validation, we performed docking trials using a BlueROV2 and an actuated dock in the OH Hinsdale Wave basin in Corvallis, OR. To obtain the relative positioning of the BlueROV2 with respect to the dock, we implemented visual servoing using fiducial markers. Different-sized markers were attached to the back panel of the dock to enable persistent visual detection at all times, during the docking operation. The front-facing camera of the BlueROV2 was calibrated using a checkerboard, to obtain the camera properties. The dock was heave-actuated with a sinusoidal oscillation that had the following properties:

- Amplitude $= 6.35\ cm/s$; Frequency $= 0.6\ Hz$
- Amplitude $= 7.62\ cm/s$; Frequency $= 0.8\ Hz$

The initial position of the vehicle was approximately $2\ m$ in front of the dock. Note that for these experiments, we only validated the performance of Oracle MPC with zero flow since it is not possible to generate currents in the facility.

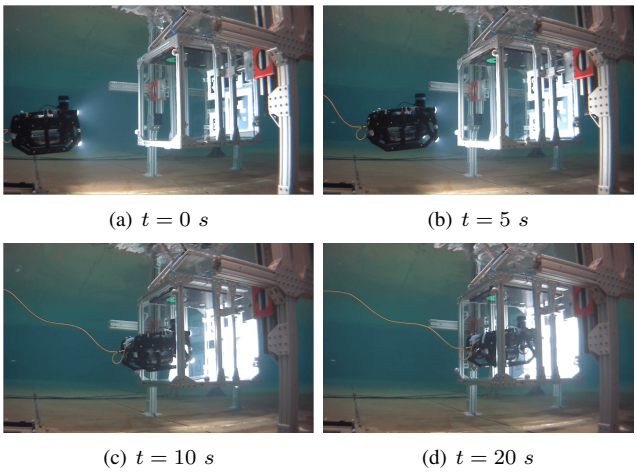

(a) $t = 0\ s$ (b) $t = 5\ s$

(c) $t = 10\ s$ (d) $t = 20\ s$

Fig. 6: Successful attempt at docking autonomously with an oscillating docking station, using fiducial markers. The sequence of images illustrates the approach and docking phase of the vehicle. The dock is actuated along the heave axis, causing it to move up and down.

B. Results and Discussion

We were able to reliably and repeatedly dock autonomously in 8 out of 11 attempts with different heave motions of the dock, using fiducial markers. Fig. 6 illustrates one such successful attempt at autonomous docking with an oscillating dock. Failures typically occurred due to the loss of fiducial tracking or the inability to avoid collisions. While the trials were performed in still conditions, these results indicate the robustness and reliability of the proposed algorithm for autonomous underwater docking in real conditions with an oscillating dock.

IX. Conclusion and Future Work

Autonomous docking is a key aspect of underwater exploration with marine vehicles as it provides power, data transmission, reduces operational costs, and increases the endurance of the vehicle. Generally, it is difficult to perform dynamic rendezvous and autonomously dock in energetic environments. To overcome this limitation, we proposed a navigation framework that couples flow state estimation into the MPC framework for optimal control of the vehicle. The simulation results demonstrate the vehicle successfully approaching the docking station while countering the influence of ocean currents along its path. The results demonstrated that both our frameworks, namely Sequential and Optimized FSE-MPC, are robust and reliable strategies for autonomous docking. Additionally, Sequential FSE-MPC was found to be computationally less expensive than Optimized FSE-MPC. Furthermore, we conducted field trials on a BlueROV2 with a dock oscillating along the heave direction and achieved a greater than 70% success rate.

Future work includes conducting field trials in energetic environmental conditions with complex dock motion. Furthermore, we intend to incorporate the effect of waves into the navigation framework presented in this paper. We also plan to look into wave-current interactions and the use of a sonar imaging sensor for improved vehicle localization and 3D reconstruction of the docking station.

REFERENCES

[1] K. Teo, E. An, and P.-P. J. Beaujean, "A robust fuzzy autonomous underwater vehicle (AUV) docking approach for unknown current disturbances," *IEEE Journal of Oceanic Engineering*, vol. 37, no. 2, pp. 143–155, 2012.

[2] J. Vaganay, P. Baccou, and B. Jouvencel, "Homing by acoustic ranging to a single beacon," in *Proc. IEEE/MTS OCEANS Conference and Exhibition*, vol. 2, pp. 1457–1462, 2000.

[3] A. S. Gadre and D. J. Stilwell, "A complete solution to underwater navigation in the presence of unknown currents based on range measurements from a single location," in *Proc. IEEE/RSJ International Conference on Intelligent Robots and Systems*, pp. 1420–1425, 2005.

[4] T. Casey, B. Guimond, and J. Hu, "Underwater vehicle positioning based on time of arrival measurements from a single beacon," in *Proc. IEEE/MTS OCEANS Conf., Vancouver, BC, Canada*, 2007.

[5] H. Singh, J. G. Bellingham, F. Hover, S. Lemer, B. A. Moran, K. Von der Heydt, and D. Yoerger, "Docking for an autonomous ocean sampling network," *IEEE Journal of Oceanic Engineering*, vol. 26, no. 4, pp. 498–514, 2001.

[6] R. S. McEwen, B. W. Hobson, L. McBride, and J. G. Bellingham, "Docking control system for a 54-cm-diameter (21-in) AUV," *IEEE Journal of Oceanic Engineering*, vol. 33, no. 4, pp. 550–562, 2008.

[7] S. Fan, B. Li, W. Xu, and Y. Xu, "Impact of current disturbances on AUV docking: Model-based motion prediction and countering approaches," *IEEE Journal of Oceanic Engineering*, vol. 43, no. 4, pp. 888–904, 2017.

[8] I. Klein and R. Diamant, "Observability analysis of dvl/ps aided ins for a maneuvering AUV," *Sensors*, vol. 15, no. 10, pp. 26818–26837, 2015.

[9] J. Osborn, S. Qualls, J. Canning, M. Anderson, D. Edwards, and E. Wolbrecht, "AUV state estimation and navigation to compensate for ocean currents," in *Proc. IEEE/MTS OCEANS Conf., Washington, DC, USA*, 2015.

[10] E. Kim, S. Fan, and N. Bose, "Estimating water current velocities by using a model-based high-gain observer for an autonomous underwater vehicle," *IEEE Access*, vol. 6, pp. 70259–70271, 2018.

[11] Z. Song and K. Mohseni, "Long-term inertial navigation aided by dynamics of flow field features," *IEEE Journal of Oceanic Engineering*, vol. 43, no. 4, pp. 940–954, 2017.

[12] Z. Song and K. Mohseni, "Concurrent flow-based localization and mapping in time-invariant flow fields," in *IEEE/RSJ International Conference on Intelligent Robots and Systems (IROS)*, pp. 7205–7210, 2019.

[13] R. Vivekanandan, D. Chang, and G. A. Hollinger, "Model predictive control for underwater vehicle rendezvous and docking with a wave energy converter," in *Proc. IEEE International Conf. on Robotics and Automation Workshop on Reliable AI for Marine Robotics: Challenges and Opportunities, virtual*, October, 2021.

[14] R. Vivekanandan, D. Chang, and G. A. Hollinger, "Flow state estimation and optimal control for autonomous underwater docking," in *Proc. University Marine Energy Research Community (UMERC) Conference, Portland, OR*, September, 2022.

[15] J. D. Hernández, E. Vidal, M. Moll, N. Palomeras, M. Carreras, and L. E. Kavraki, "Online motion planning for unexplored underwater environments using autonomous underwater vehicles," *Journal of Field Robotics*, vol. 36, no. 2, pp. 370–396, 2019.

[16] R. Findeisen and F. Allgöwer, "An introduction to nonlinear model predictive control," in *Benelux meeting on systems and control*, vol. 11, pp. 119–141, 2002.

[17] L. Medagoda and S. B. Williams, "Model predictive control of an autonomous underwater vehicle in an in situ estimated water current profile," in *Proc. IEEE/MTS OCEANS Conf., Yeosu, Korea*, 2012.

[18] D. C. Fernández and G. A. Hollinger, "Model predictive control for underwater robots in ocean waves," *IEEE Robotics and Automation Letters*, vol. 2, no. 1, pp. 88–95, 2016.

[19] Y. Zhang, X. Liu, M. Luo, and C. Yang, "MPC-based 3-D trajectory tracking for an autonomous underwater vehicle with constraints in complex ocean environments," *Ocean Engineering*, vol. 189, p. 106309, 2019.

[20] J. Wallen, N. Ulm, and Z. Song, "Underwater docking system for a wave energy converter based mobile station," in *Proc. IEEE/MTS OCEANS Conf., Seattle, WA*, 2019.

[21] Z. Yan, P. Gong, W. Zhang, and W. Wu, "Model predictive control of autonomous underwater vehicles for trajectory tracking with external disturbances," *Ocean Engineering*, vol. 217, p. 107884, 2020.

[22] Y. Cao, B. Li, Q. Li, A. A. Stokes, D. M. Ingram, and A. Kiprakis, "A nonlinear model predictive controller for remotely operated underwater vehicles with disturbance rejection," *IEEE Access*, vol. 8, pp. 158622–158634, 2020.

[23] D. Chang, M. Johnson-Roberson, and J. Sun, "An active perception framework for autonomous underwater vehicle navigation under sensor constraints," *IEEE Transactions on Control Systems Technology*, vol. 30, no. 6, pp. 2301–2316, 2022.

[24] T. I. Fossen, *Handbook of marine craft hydrodynamics and motion control*. John Wiley & Sons, 2011.

[25] C.-J. Wu, *6-DOF modelling and control of a remotely operated vehicle*. PhD thesis, Flinders University, College of Science and Engineering., 2018.

[26] R. G. Dean and R. A. Dalrymple, *Water wave mechanics for engineers and scientists*, vol. 2. World Scientific Publishing Company, 1991.

[27] J. A. E. Andersson, J. Gillis, G. Horn, J. B. Rawlings, and M. Diehl, "CasADi – A software framework for nonlinear optimization and optimal control," *Mathematical Programming Computation*, vol. 11, no. 1, pp. 1–36, 2019.

[28] S. C. Shadden, F. Lekien, and J. E. Marsden, "Definition and properties of lagrangian coherent structures from finite-time lyapunov exponents in two-dimensional aperiodic flows," *Physica D: Nonlinear Phenomena*, vol. 212, no. 3-4, pp. 271–304, 2005.